

Comparative observations on the squamous-columnar junction of Von Ebner's glandular duct at the bottom of vallate papillae in dogs, rats, mice and human

Xinyu Chen¹⁻⁴, Lin Luo¹⁻⁴, Pengning Chen¹⁻⁴, Guanxi Chen¹⁻⁴, Qizhang Yan¹⁻⁴, Bosen Zhou¹⁻⁴, Nengming Liu¹⁻⁴, Ping Ruan⁵, Dahai Yu⁶

¹College of Stomatology, Hospital of Stomatology, Guangxi Medical University, Nanning, China

²Guangxi Key Laboratory of Oral and Maxillofacial Rehabilitation and Reconstruction, Nanning, China

³Guangxi Clinical Research Centre for Craniofacial Deformity, Nanning, China

⁴Guangxi Health Commission Key Laboratory of Prevention and Treatment for Oral Infectious Diseases, Nanning, China

⁵Department of Pathology, Ruikang Hospital Affiliated to Guangxi University of Chinese Medicine, Nanning, China

⁶Department of Stomatology, The First Affiliated Hospital of Guangxi Medical University, Nanning, China

[Received: 2 August 2023; Accepted: 23 October 2023; Early publication date: 31 October 2023]

Background: This paper aims to comparatively observe similarities of squamous-columnar junction (SCJ) at the opening of Von Ebner's glandular ducts at the vallate papillae in dogs, mice, rats and humans, lay a foundation for the selection of the model in future study of the carcinogenesis in SCJ at vallate papillae.

Materials and methods: The localization of the vallate papillae in three laboratory animals and humans was comparatively observed. The differences of SCJ at vallate papillae were comparatively observed by alcian blue, immunohistochemistry and H&E staining.

Results: Anatomically, the canine vallate papillae were most similar to those of humans in location, whereas mice and rats only had a single, Ω-shaped, vallate papilla lying directly anterior to the posterior border of the intermolar eminence. In histology, the SCJ of dogs lacked a transition zone similar to that of the human SCJ, and there was glandular epithelium secreting acidic mucus at the opening of the rats' Von Ebner's glandular ducts. All of this suggested that the histological structure of SCJ in rats and dogs is more distinct from that of humans, whereas the histological structure of SCJ at vallate papilla in mice was more similar.

Conclusions: The structure of SCJ at vallate papilla in mice is most similar to that of humans, so we conclude that mouse is the most suitable model for studying tumorigenesis in SCJ at vallate papillae in these three common laboratory animals. (Folia Morphol 2024; 83, 3: 667–679)

Keywords: squamous-columnar junction, SCJ, Von Ebner's glands, Vallate papillae

Address for correspondence: Dahai Yu, Department of Stomatology, The First Affiliated Hospital of Guangxi Medical University, No. 6 Shuangyong Road, Qingxiu District, Nanning 530021, China; tel: +86-13877123499, e-mail: yudahai813@sr.gxmu.edu.cn

This article is available in open access under Creative Common Attribution-Non-Commercial-No Derivatives 4.0 International (CC BY-NC-ND 4.0) license, allowing to download articles and share them with others as long as they credit the authors and the publisher, but without permission to change them in any way or use them commercially.

INTRODUCTION

Oropharyngeal squamous cell carcinoma (OPSCC), which comprises cancers of the tonsils, base of tongue, soft palate and posterior walls of the oropharynx, is a significant subset of head and neck squamous cell carcinoma (HNSCC) [16, 20]. OPSCC arises most commonly from the palatine and lingual tonsils [6, 24]. As a major risk factor for OPSCC [4, 25, 31], human papilloma virus (HPV) preferentially targets the unique reticulated squamous epithelium lining the tonsillar crypts and fissures structures of the basal layer, and this highly specialized epithelium is the critical reason why HPV-mediated OPSCC is mostly located in these specific sites [13]. Due to the reticulated epithelium, previous studies on the carcinogenesis of OPSCC have mainly focused on the lingual and palatine tonsils, and there has been no correlational study on other oropharyngeal regions.

The transition zone between different types of epithelium is now known to be a high hazard area for precancerous lesions and carcinomas [12, 22, 33]. In the cervix and anus, the squamous-columnar junction (SCJ), as an HPV-susceptible transition zone, has been extensively studied. At present, the SCJ, which resides at the boundary of the ectocervix and endocervix, is widely recognized as a prime target of HPV infection and subsequent carcinoma development [11]. And the large majority of high-grade squamous intraepithelial lesions and uterine cervical cancers arise in this area [18]. In the anus, SCJ is also strongly associated with the development of low-grade and high-grade anal intraepithelial neoplasia (AIN) and anal cancer caused by HPV [26]. Furthermore, the conversion from SCJ to transformation zone is not limited to HPV infection. In the gastroesophageal junction, a similar conversion process can be caused by chronic gastroesophageal reflux disease, which can lead to the transformation of the stratified squamous epithelium into columnar epithelium to form Barrett's oesophagus and eventually carcinoma [9]. In previous study, we have found the transition zone, which is similar to SCJ that can lead to the development of cervical and anal carcinomas, at the vallate papillae of human and mouse. Furthermore, we have also found structurally similar transformation zones following squamous metaplasia in vallate papillae to those following squamous intraepithelial lesions in the cervix. And we have also successfully induced the conversion of SCJ at the opening of Von Ebner's glandular duct in the 4-nitroquinoline-1-oxide (4-NQO) -treated mouse model of oral squamous cell carcinomas [5]. Therefore, We have speculated that

SCJ of Von Ebner's glands maybe a significant origin of squamous cell carcinomas in base of the tongue.

At present, there were very few studies on how such particular structures at the opening of Von Ebner's glandular duct can be stimulated to take place squamous metaplasia to form transformation zones and further carcinogenesis. Moreover, due to the restrictions of medical ethics, it is difficult to obtain tissue samples at various stages of carcinoma at SCJ of Von Ebner's gland in clinical practice. Therefore, it is in great need of a appropriate animal model for research. This study aims to comparatively observe similarities of SCJ at the opening of Von Ebner's glandular ducts at the vallate papillae (Known as vallate papillae in rodents [14]) in three common laboratory animals in the field of stomatology (Dogs, mice and rats) using immunohistochemistry staining with SCJ markers [Cytokeratin 7(CK7), Cytokeratin 5(CK5), and Tumour Protein P63(p63)] [17, 19, 23, 33], and compare with human beings'. And the serous Von Ebner's glands are determined by alcian blue staining. On this basis, we will preliminarily determine the similarity of the histological structures of each animal to that of human and lay the foundation for the selection of the model in subsequent animal experiments.

MATERIALS AND METHODS

Sample collection

All procedures were conducted according to the guidelines assigned by The First Affiliated Hospital of Guangxi Medical University ethical review committee, China (Approval No. 2023-E055-01).

Tongues from mice (n = 20), rats (n = 20), and dogs (n = 10) were obtained after the euthanasia of animals that had been used in other studies. The localization of the vallate papillae was demonstrated by anatomical dissection. Photographs of fresh tongue tissues were taken using a digital camera (Canon EOS 300D, Diegem, Belgium).

Ten vallate papillae of mice and rats were respectively obtained in the sagittal and coronal planes, and 10 vallate papillae of dogs were obtained. These samples were fixed in 4% buffered paraformaldehyde at room temperature for 24 hours. dehydrated in a tissue processor (Microm STP420D, Prosan, Merelbeke, Belgium), and embedded in paraffin using an embedding station (Microm EC350-1 and 350-2, Prosan, Merelbeke, Belgium).

Paraffin samples of 10 cases of tongue squamous cell carcinomas that had been excised in surgery and

diagnosed by pathology between September 2021 and May 2022 from the Affiliated Stomatological Hospital of Guangxi Medical University were selected, and the vallate papillae of normal tissues around the carcinomas were resected for further experimental study.

Five 4- μ m serial sections were obtained from each sample.

Haematoxylin and eosin staining

The paraffin was removed from the samples using four changes of xylene for 5 min each. The slides were hydrated in gradient ethanol and rinsed three times in tap water. The samples were stained for 7 min in Harris' haematoxylin solution, and the slides were rinsed three times in tap water. Then the samples were stained in eosin solution for 2 min, the slides were rinsed three times in tap water, conventionally dehydrated in alcohol, and cleared in three changes of xylene for 2 min each. Finally, each slide was sealed with neutral balsam.

Immunohistochemistry for CK7, CK5 and p63

For immunostaining, 4 μ m longitudinal sections of the paraffin-embedded samples were kept at 60°C for 3 h in the oven and then followed by deparaffinizing with xylene and hydrating with an ethanol gradient (100–70%), washed three times in distilled water, heated in a pressure cooker in Tris-EDTA (pH = 9.0) to retrieve antigenic activity, and then cooled at room temperature. Endogenous peroxidase activity was inhibited by incubation with 3% hydrogen peroxide for 20 minutes at 37°C. After nonspecific reactions had been blocked, the sections were incubated overnight at 4°C with primary antibodies: CK5 (OT11C7, 1:200; ZSGB-BIO, Beijing, China), CK7 (EP16, 1:200; ZSGB-BIO, Beijing, China) and p63 (4A4+UMAB4, 1:200; ZSGB-BIO, Beijing, China). The next day, the sections were rinsed and incubated with biotinylated goat anti-mouse immunoglobulin G (IgG) for 20 minutes at 37°C. Careful rinses were performed with several changes of PBS buffer between each stage of the procedure. Then the colour was developed with 3,3'-diaminobenzidine (DAB) and the sections were counterstained with haematoxylin. Finally, the slides were conventionally dehydrated in alcohol, cleared in xylene, and each slide was sealed with neutral balsam.

Alcian blue staining

The paraffin was removed from the samples for alcian blue staining in four changes of xylene for 5 min

each. The slides were hydrated in gradient ethanol, rinsed the slides three times in tap water. Then the slides were equilibrated in 5% acetic acid for 3 min, stained in alcian blue solution (PH = 2.5) for 30 min, and rinsed in running tap water for at least 5 min. The slides were then counterstained for 5–10 min with nuclear fast red staining solution before being rinsed for at least 1 min in running tap water. Finally, the slides were conventionally dehydrated in alcohol, cleared in xylene, and sealed with neutral balsam.

Microscopic observation

The similarities of SCJ at the opening of Von Ebner's glandular duct at the vallate papilla in humans, dogs, mice and rats were comparatively observed with haematoxylin and eosin (H&E), immunochemical and alcian blue staining, and all slides were examined by light microscopy (Eclipse Ni-U, Nikon, Tokyo, Japan).

RESULTS

Comparison of anatomical location of contoured papillae in rats, mice and dogs

An eminence was seen at the junction of the anterior two-thirds and the posterior one-third of the dorsum of the tongue, called the inter molar eminence. Its posterior border resembled human's sulcus terminalis, and a single, Ω -shaped, vallate papilla lied directly anterior to it. The anatomical structure of the rat's tongue was similar to that of the mouse, A single vallate papilla of rat was also located in the slightly anterior median of the posterior border of the inter molar eminence. The anatomical location of the canine vallate papilla was similar to that of the human, Two or three papillae were arranged close to each other forming a line on either side, and the two lines converged from front to back on the lingual surface. Vallate papillae were circular, about 4–6 in number. Each papilla measured 2–3 mm in diameter and was surrounded by a deep wide vallate papilla furrow, and the lingual mucosa outside the vallate papilla furrow was slightly elevated, forming the papilla vallate's boundary (Fig. 1).

Observation of SCJ in human vallate papillae with H&E, immunohistochemical and alcian blue staining

Taste buds were only visible in the lateral wall of the vallate papilla furrow in human vallate papillae. The transition zone of SCJ was present closer to the bottom of the furrow, approximately 10–20 cells in size,

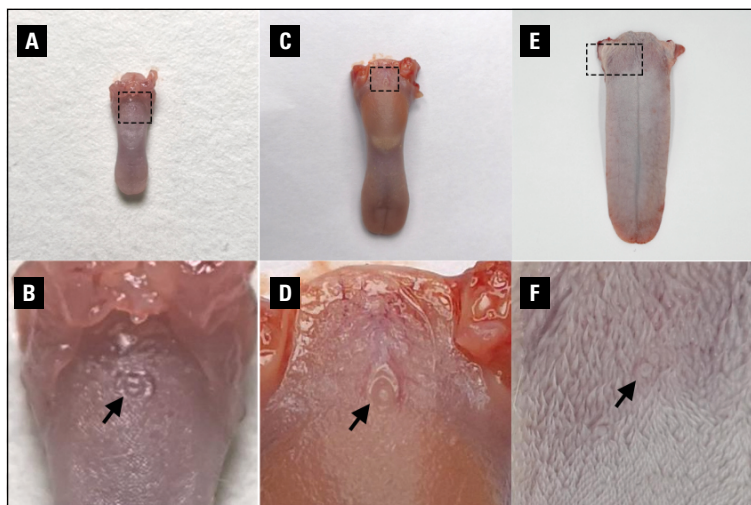


Figure 1. Anatomic localization of vallate papillae in mouse, rat and dog. **A, B.** Total tongue and vallate papilla (arrow) of mice; **C, D.** Total tongue and vallate papilla (arrow) of rats; **E, F.** Total tongue and vallate papilla (arrow) of dogs. (**B, D, F** corresponds to the structure in **A, C, E** dotted space respectively).



Figure 2. H&E staining of SCJ in human vallate papillae. Pseudostratified columnar epithelium could be seen in the columnar epithelial zone, it gradually migrated as a single layer of columnar epithelium at the transition zone and was always located above basal-like cells; stratified squamous epithelium could be seen in the squamous epithelial zone. H&E — haematoxylin and eosin; SCJ — squamous-columnar junction.

a single layer of columnar epithelium migrating from 3~4 layers of pseudostratified columnar epithelium in the columnar epithelial zone of the duct was observed and always located above basal-like cells, which were finally replaced by non-keratinized stratified squamous epithelium. The squamous epithelial zone beside the SCJ consisted of 7~8 layers of non-keratinized stratified squamous epithelium, which was gradually in transition to the keratinized squamous epithelium as it got further away from the transition zone. Intercellular bridges could also be seen in the transitional zone and stratified squamous epithelium (Fig. 2). The expression of CK7 could be seen in the taste buds of the squamous epithelial zone. In addition, CK7 positive monolayer columnar epithelia were found in the surface layer of SCJ. CK5 was expressed in the squamous epithelial zone as well as the lower layer of the transition zone. The consecutive expression of p63 could be seen in the basal layer of the squa-

mous epithelial zone and the transition zone (Fig. 3). The Von Ebner's glands around vallate papillae had serous acini, each of which consisted of several cells with different shapes such as oval, spherical and pyramidal. And they were embedded in the skeletal muscles and submucosa of the posterior dorsum of the tongue, surrounding the single vallate papilla. Striated, intercalated and stratified columnar ducts could be seen in Von Ebner's glands. The reaction of serous acini of the Von Ebner's glands to the alcian blue staining was negative (Fig. 4).

Observation of SCJ in canine vallate papillae with H&E, immunohistochemical and alcian blue staining

In dogs, the duct of Von Ebner's glands opened at the base of the vallate papilla furrow. Multiple taste buds were located in the walls of their furrows in vallate papilla. The keratinized stratified squamous

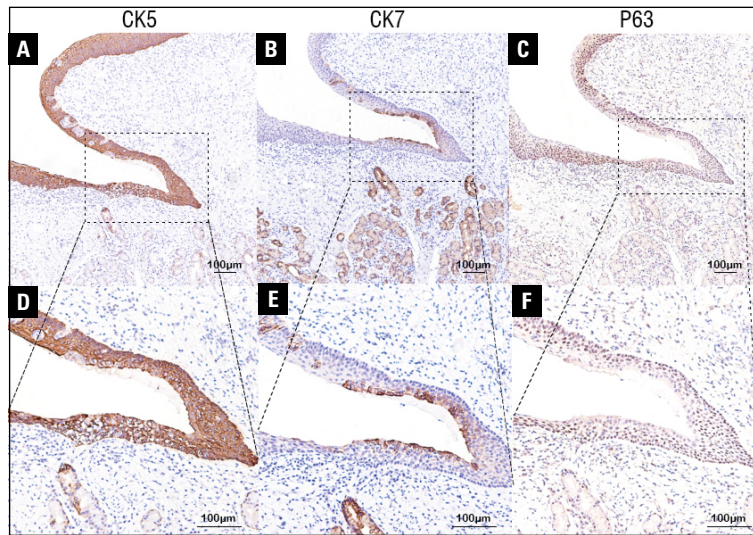


Figure 3. IHC staining of SCJ in human vallate papillae. The expression of CK5 could be seen in the squamous epithelial zone and the lower layer of the transition zone (A, D); CK7 positive monolayer columnar epithelia could be seen in the surface layer of SCJ (B, E); p63 was consecutively expressed in the basal layer of the squamous epithelial zone and transition zone (C, F). SCJ is shown in the dotted line area. IHC — immunohistochemistry; SCJ — squamous-columnar junction.

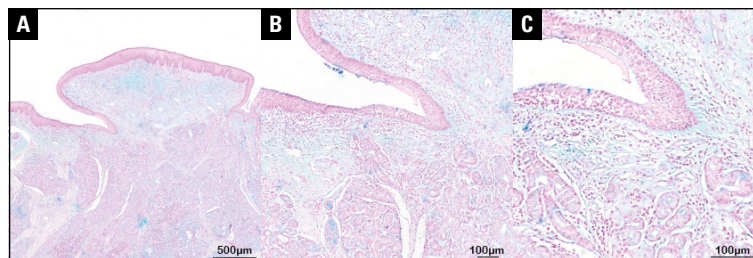


Figure 4. Alcian blue staining of glands near human vallate papillae. Image showed negative reaction of serous acini to alcian blue (pH = 2.5) staining.

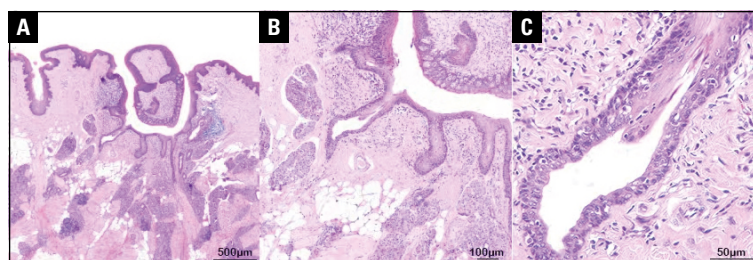


Figure 5. H&E staining of SCJ in canine vallate papillae. H&E staining shows the pseudostratified columnar epithelium was directly connected to the stratified squamous epithelium. H&E — haematoxylin and eosin; SCJ — squamous-columnar junction.

epithelium lining the wall of the vallate papilla furrow was directly connected to the pseudostratified columnar epithelium at the furrow's base, lacking the transition zone seen at the human SCJ (Fig. 5). CK7 was found in the entire columnar epithelial zone as well as taste buds in the squamous epithelial zone. CK5 was expressed in the whole squamous epithelial zone and the external muscular layer epithelium

of the acini. CK5-positive ductal epithelial reserve cells were found in the columnar epithelial zone. The consecutive expression of p63 could be seen in the basal layer of the squamous epithelial zone and the columnar epithelial zone (Fig. 6). Von Ebner's glands around vallate papillae, which were composed exclusively of serous acinar epithelium and interlobular excretory ducts, were divided into several lobules by

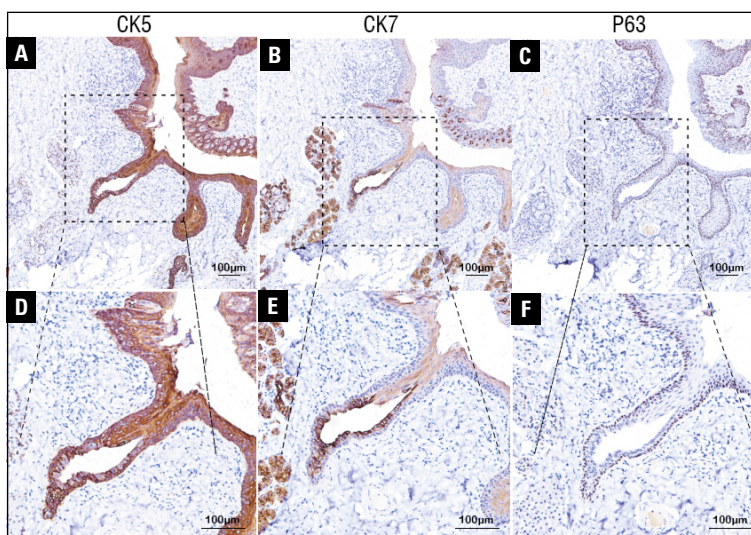


Figure 6. IHC staining of SCJ in canine vallate papillae. CK5-positive ductal epithelial reserve cells were found in the columnar epithelial zone (A, D), and the columnar epithelial zone of full-layer CK7 expression was directly linked to the squamous epithelial zone of full-layer CK5 expression (B, E). The consecutive expression of p63 could be seen in the basal layer of the squamous epithelial zone and the columnar epithelial zone (C, F). IHC — immunohistochemistry; SCJ — squamous-columnar junction.

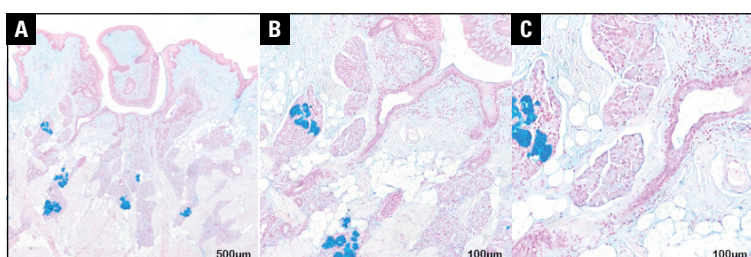


Figure 7. Alcian blue staining of SCJ in canine vallate papillae. Alcian blue staining showed negative reaction in Von Ebner's glands, in which alcian blue staining positive mucous acini were scattered. SCJ — squamous-columnar junction.

connective tissue septa. The reaction of serous acini of the Von Ebner's glands to the alcian blue staining was negative. Scattered Weber glands that respond positively to alcian blue staining were seen in Von Ebner's acinar (Fig. 7).

Observation of SCJ in mice's vallate papillae with H&E, immunohistochemical and alcian blue staining

The duct of mice's Von Ebner's glands opened below the taste buds at the bottom of the vallate papilla furrow. The keratinized stratified squamous epithelium lining the wall of the vallate papilla furrow was gradually in transition to the non-keratinized stratified squamous epithelium after entering the duct segment and connected to the transition zone of the duct. The transition zone consisted of a single layer of columnar epithelium on the luminal side and basal-like cells beneath it. The columnar epithelial

zone at the start of the duct was composed of 2–3 layers of pseudostratified columnar epithelium and was connected to the serous acini. Coronal sections of the vallate papilla in mice revealed a fungiform form similar to that of humans, as well as a furrow on both sides. Taste buds were found to be distributed not only in the wall of the vallate papilla furrow but also at the furrow's base, and Von Ebner's glandular ducts opened below the taste buds at the base of the vallate papilla furrow (Fig. 8). The expression of CK7 could be seen in the taste buds of the squamous epithelial zone. The surface layer of the transition zone also found to contained CK7-positive monolayer columnar epithelia. And CK7 was expressed in the whole columnar epithelial zone at the start of the duct. CK5 was expressed in the whole squamous epithelial zone, the external muscular layer epithelium of the acini and the lower layer of transition zone. The consecutive expression of p63 could be seen in the basal layer of

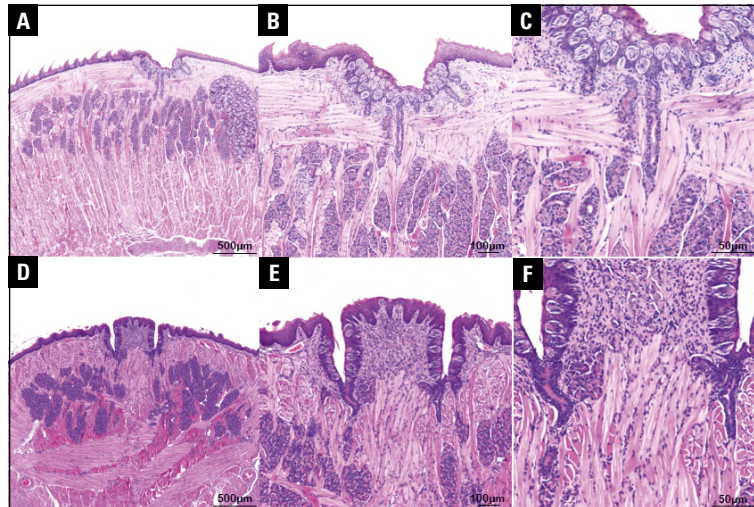


Figure 8. H&E staining of SCJ in mouse's vallate papilla. (A–C in sagittal plane; D–F in coronal plane) The transitional zone was located in the middle and upper segment of the duct and consisted of a single layer of columnar epithelium on the luminal side and basal-like cells beneath it (A–C). Coronal sections of the vallate papilla in mice showed a fungiform form similar to that of humans, and the vallate papilla furrow on both sides (D–F). H&E — haematoxylin and eosin; SCJ — squamous-columnar junction.

the squamous epithelial zone, transition zone and the columnar epithelial zone (Fig. 9). The Von Ebner's glands at vallate papilla were composed exclusively of serous acini and interlobular excretory ducts. Serous acini of Von Ebner's glands were negative for alcian blue staining. Weber glands were found along the lingual border side and the base of the tongue side of the vallate papilla, which were strongly positive for alcian blue staining (Fig. 10).

Observation of SCJ in rats' vallate papilla with H&E, immunohistochemical and alcian blue staining

The structure of SCJ in rats' Von Ebner's glandular ducts is basically similar to that of mice. But rats' Von Ebner's glandular ducts were more tortuous. Moreover, the duct of muco-secreting Weber's glands and Von Ebner's glands jointly opened at the bottom of the vallate papilla furrow (Fig. 11). The expression of CK7, CK5 and p63 was similar to that of mice (Fig. 12). Von Ebner's glands were divided into several lobules by connective tissue septa and their serous acini were negative for alcian blue staining. Alcian blue-positive Weber glands were found at the opening of Von Ebner's glandular ducts and the lingual border side and the base of the tongue side of the vallate papilla. And there were glandular epithelium secreting acidic mucus at the opening of Von Ebner's glandular duct, which was strongly positive for alcian blue staining (Fig. 13).

DISCUSSION

Current studies of OPSCC have mainly focused on the tonsils, whereas rats and mice are rarely used in studies of OPSCC because their oropharynx (including the root of the tongue) lacks the Waldeyer's ring similar to the human tonsils and other oropharyngeal lymphoid tissues (It means the lack of unique reticulated squamous epithelium which lines the crypts and fissures structures of tonsils) [14]. The SCJ of vallate papilla has attracted much attention as a possible origin of OPSCC, and the lack of relevant models is an urgent issue that we need to address now.

Mice, rats and dogs are commonly used as laboratory animals in the field of stomatology and are widely used in the study of oral squamous cell carcinoma [3, 10, 29]. This study attempts to explore the possibility of constructing an OPSCC research model based on these three common oral squamous cell carcinoma animal models through histological observation and comparison.

In dogs, images showed that Von Ebner's glandular ducts lacked a transition zone similar to that of the human SCJ. At the opening of Von Ebner's glandular ducts at the base of the furrow, the keratinized stratified squamous epithelium lining the wall of the vallate papilla furrow was directly connected to the pseudostratified columnar epithelium. In addition, alcian blue staining showed the presence of mucous Weber glands near Von Ebner's glands, but no direct opening at the vallate papillae.

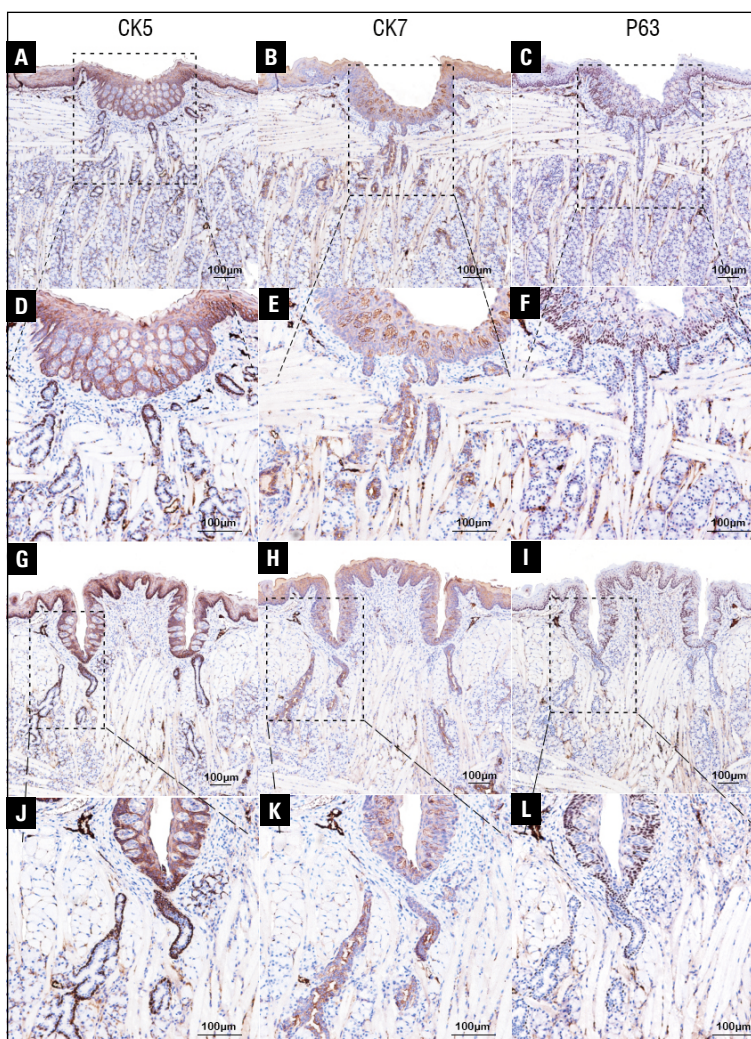


Figure 9. IHC staining of SCJ in mouse's vallate papilla. (A–F in sagittal plane; G–L in coronal plane) CK5 was expressed in the whole squamous epithelial zone and the lower layer of the transition zone (A, D, G, J). CK7 was expressed in the whole columnar epithelial zone at the start of the duct and the taste buds of the squamous epithelial zone and CK7 positive monolayer columnar epithelia were present in the surface layer of transition zone (B, E, H, K). p63 was expressed consecutively in the basal layer of the squamous epithelial zone, transition zone and the columnar epithelial zone (C, F, I, L). IHC — immunohistochemistry; SCJ — squamous-columnar junction.

The structures around SCJ of Von Ebner's glandular ducts in rats and mice are similar. Compared with human, the taste buds of rats and mice not only existed in the lateral wall of the vallate papilla furrow, but also at the base of the vallate papilla furrow. The Von Ebner's glandular duct of rats and mice opened below the taste buds at the base of the vallate papilla furrow. And the presence of CK5-positive ductal epithelial reserve cells (These cells have the features of stem cells, which can repair and regenerate ductal and acinar cells but also have the potential to transform into cancer stem cells [28]) in the SCJ of their Von Ebner's glands similar to that in the SCJ of the human vallate papilla was also observed. After observation, we found that it is easier to observe the

complete structure of the Von Ebner's glandular duct in rats and mice through sagittal plane. Although the coronal plane can observe the structure of fungiform vallate papilla similar to that of humans, it is difficult to obtain the complete structure of the Von Ebner's glandular duct. If researchers want to study SCJ of the Von Ebner's glandular duct through rats and mice, the sagittal plane can obtain better observation effect.

In addition, images also showed the presence of alcian blue positive Weber's glands around Von Ebner's glands in rats and mice. Weber's glands are mucous with serous demilunes, lying lateral and posterior to the Von Ebner's gland associated with the vallate papilla, and they are very close to each other. There are even scattered mucous acini of Weber's

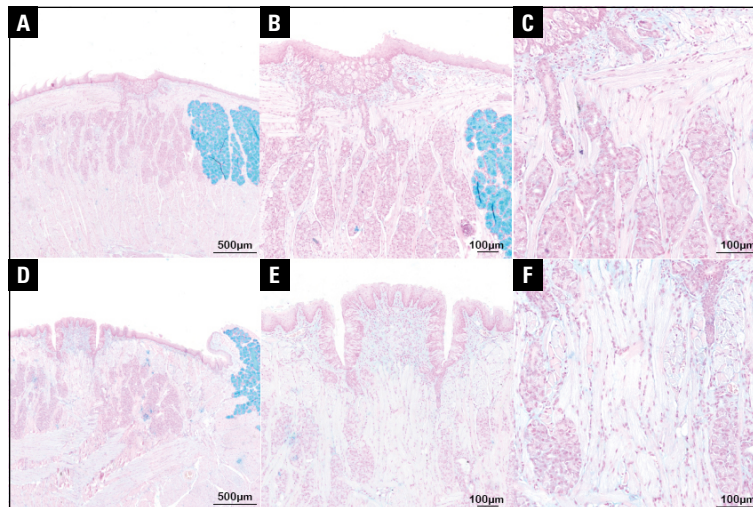


Figure 10. Alcian blue staining of SCJ in mouse's vallate papilla. (A–C in sagittal plane; D–F in coronal plane) Alcian blue staining showed negative reaction to serous acini of Von Ebner's glands. Alcian blue positive mucous acini were found along the lingual border side and the base of the tongue side of the vallate papilla. SCJ — squamous-columnar junction.

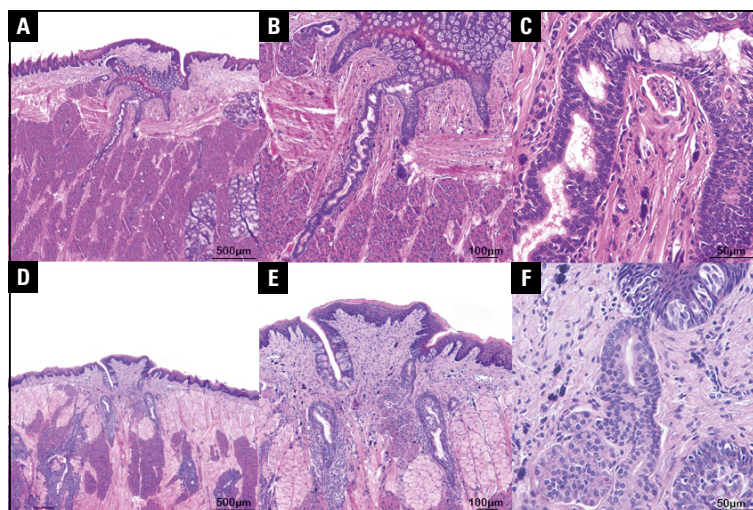


Figure 11. H&E staining of SCJ in rat's vallate papilla. (A–C in sagittal plane; D–F in coronal plane). The transitional zone was located in the middle and upper segment of the duct and consisted of a single layer of columnar epithelium on the luminal side and basal-like cells beneath it. the duct of muco-secreting Weber's glands and Von Ebner's glands jointly opened at the bottom of the vallate papilla furrow (A–C). Coronal sections of the vallate papilla in mice showed a fungiform form similar to that of humans, and the vallate papilla furrow on both sides (D–F). H&E — haematoxylin and eosin; SCJ — squamous-columnar junction.

glands among the serous acini of Von Ebner's gland. Weber's glands, however, lack striated and stratified columnar ducts, and the tubulo-acini drain abruptly into short terminal ducts composed of stratified squamous epithelium [30]. In most rat samples, it could be noted that there were extra glandular epithelium secreting acidic mucus at the opening of Von Ebner's glandular ducts at the base of the vallate papilla furrow, but almost nothing similar had been observed in mice (Fig. 14).

Some research suggests that this may be related to the fact that the Weber's glands and Von Ebner's glands in rats are more closely located and their excretory ducts converge into a duct at the bottom of the vallate papilla furrow. In human vallate papillae, serous Von Ebner's glands are the main glands, while Weber's glands are mainly located in lingual tonsil, the lateral and posterior to the Von Ebner's gland associated with the vallate papilla. And there are no reports that Weber's glands open at the bottom of

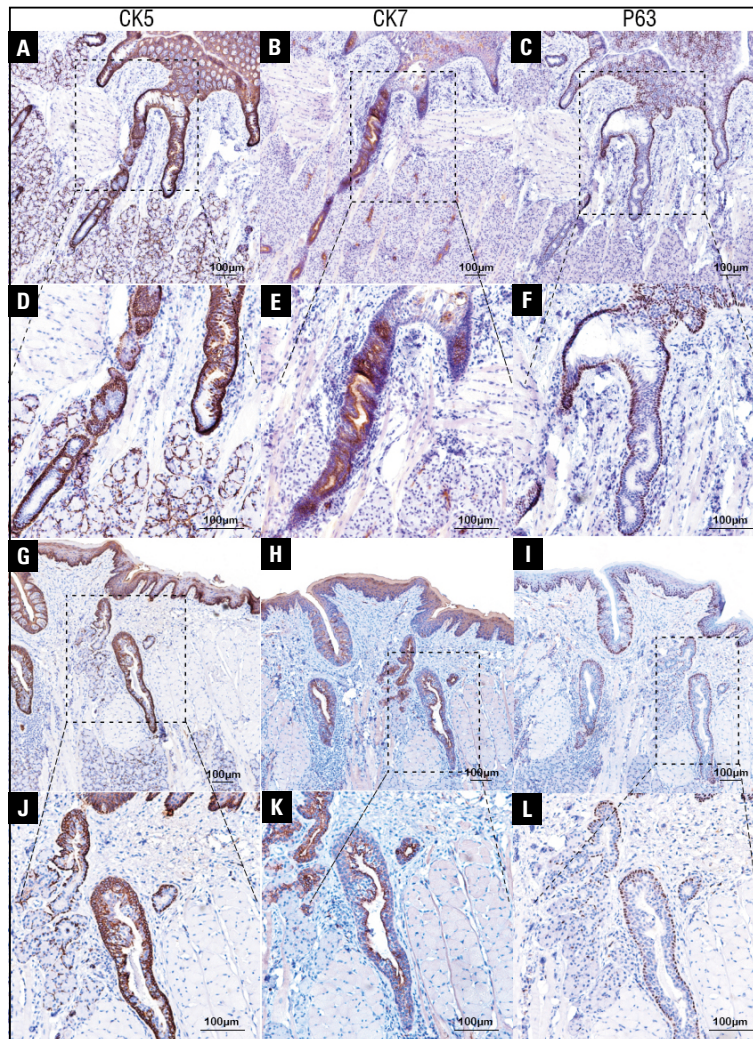


Figure 12. IHC staining of SCJ in rat's vallate papilla. (A–F in sagittal plane; G–L in coronal plane) CK5 was expressed in the whole squamous epithelial zone and the lower layer of the transition zone (A, D, G, J). CK7 was expressed in the whole columnar epithelial zone at the start of the duct and the taste buds of the squamous epithelial zone and CK7 positive monolayer columnar epithelia was present in the surface layer of transition zone (B, E, H, K). p63 was expressed consecutively in the basal layer of the squamous epithelial zone, transition zone and the columnar epithelial zone (C, F, I, L). IHC — immunohistochemistry; SCJ — squamous-columnar junction.

vallate papilla furrow. Therefore, we suggest that the histological structure near SCJ of Von Ebner's glandular duct in mice is more similar to that in humans than in rats.

Besides, the epidemiologic features of OPSCC have changed dramatically in the past decades. The number of OPSCC associated with smoking, alcohol abuse and poor oral hygiene has declined sharply, while the incidence of HPV-associated OPSCC has steadily increased globally. Oropharynx now surpasses the cervix as the most common site for HPV-associated cancers in the United States, and analogous tendencies have been observed in Europe and Asia [31]. Nowadays, HPV infection has become the most important hazard factor for OPSCC, and some studies have indicated

that the increase in oropharyngeal cancer around the world is attributable to HPV. Therefore, animal models that can simulate the carcinogenesis of HPV infection in the oropharynx will provide great value for studying the development and treatment of these cancers.

HPV is an infectious pathogen, and sexual contact is its dominant mode of transmission. Due to the dependence of the HPV life cycle on the differentiation programme of keratinocytes [21] and the strict species-specificity of HPV to not infect any other host than their natural one even in experimental conditions [2], it is difficult to establish in vitro models of HPV infection. In the course of HPV-associated carcinogenesis, E6 and E7, as the major HPV oncoproteins, are key factors in maintaining the malignant

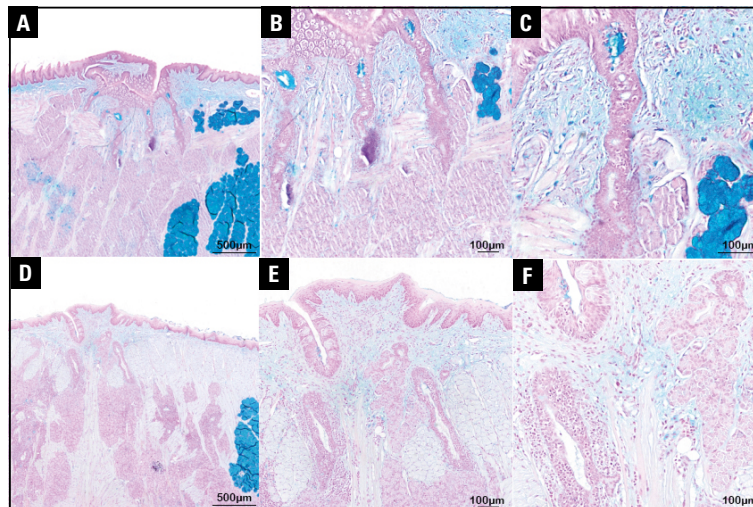


Figure 13. Alcian blue staining of SCJ in rat's vallate papilla. (A–C in sagittal plane; D–F in coronal plane). Alcian blue staining showed negative reaction to serous acini of Von Ebner's glands, and alcian blue positive mucous acini were found at the opening of Von Ebner's glandular ducts and the lingual border side and the base of the tongue side of Von Ebner's glands. And there were alcian blue positive glandular epithelium at the opening of Von Ebner's glandular duct.

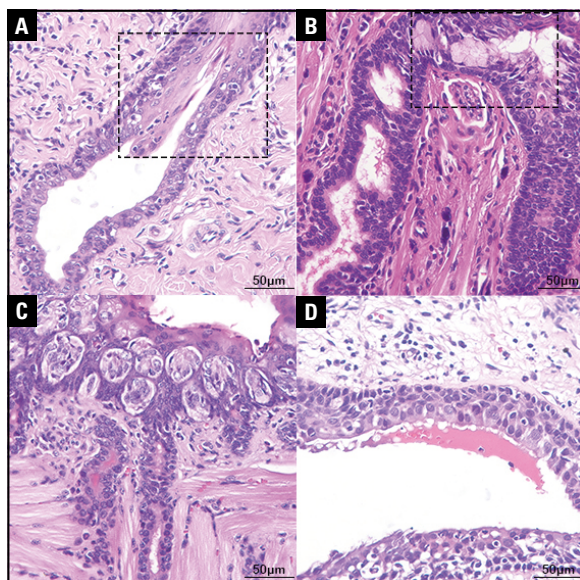


Figure 14. Comparative observations on the SCJ of Von Ebner's gland in dogs, rats, mice and human. In dog, Von Ebner's glandular ducts lacked a transition zone similar to that of the human SCJ. In rat, there were glandular epithelium secreting acidic mucus at the opening of the Von Ebner's glandular duct. The structures near the SCJ in mice were more similar to those in human than in dogs and rats. SCJ — squamous-columnar junction.

phenotype of HPV-positive cancer cells [8, 32]. With the development of genetic technology, genetically engineered mice have provided valuable insights into the carcinogenic properties of various human tumour viruses [15]. To further explore the role of HPV in carcinogenesis, a transgenic mouse model carrying the

entire HPV16 early genomic region under the control of the Keratin-14 promoter and a spontaneous HPV16 E6/E7-expressing head and neck squamous cell carcinoma model in HLA-A2 transgenic mice have been successfully created and put into use [7, 27]. The use of these mouse models has made a remarkable contribution to our understanding of how HPV directly causes cancer in humans. In addition, the mouse has its own specific papillomavirus — mouse papillomavirus (MmuPV1), which is capable of infecting laboratory mice. Some scholars have developed an efficient system using MmuPV1 to generate dysplastic oropharyngeal lesions, including tumours, in the soft palate and the base of the tongue of two immune-deficient strains of mice [1]. This HPV-infection-based mouse model of oropharyngeal tumorigenesis can better reproduce the entire process of papillomaviruses from infection to tumorigenesis, which will facilitate the study of oropharyngeal tumorigenesis and potential treatments. In contrast, the specificity of the histological structure and the sensitivity of genetic engineering techniques in rats and dogs make it more difficult to establish HPV-related animal research models that can reproduce the whole process of papillomaviruses from infection to tumorigenesis at Von Ebner's glands in the base of the tongue.

CONCLUSIONS

Among three animals — dogs, rats, and mice which are commonly used as laboratory animals in the

field of stomatology, the structure of SCJ of mouse's Von Ebner's glandular ducts is most similar to that of human. Together with the mature application of genetic engineering techniques in mice and the specific advantages of the MmuPV1 infection mouse model, we argue that mouse the most suitable animal for studying tumorigenesis in SCJ at the opening of Von Ebner's glandular duct at the base of the vallate papilla furrow among these three animals.

ARTICLE INFORMATION AND DECLARATIONS

Data availability statement

Data available on request from the authors. The data that support the findings of this study are available from the corresponding author upon reasonable request (All data generated or analysed during this study are included in this published article).

Ethics statement

This paper fully considered and protected the rights and interests of the study objects. It meets the criteria of Ethical Review Committee. The Medical Ethics Committee of First Affiliated Hospital of Guangxi Medical University has approved the protocol (approval number: 2023-E055-01).

Funding

This work was supported by This study was supported by the Natural Science Foundation of China (Grant No. 81360407) and the Guangxi Natural Science Foundation (Grant No. 2016GXNSFDA380002).

Conflict of interest

The authors declare that they have no known competing financial interests or personal relationships that could have appeared to influence the work reported in this paper.

REFERENCES

1. Bilger A, King RE, Schroeder JP, et al. A mouse model of oropharyngeal papillomavirus-induced neoplasia using novel tools for infection and nasal anesthesia. *Viruses*. 2020; 12(4), doi: [10.3390/v12040450](https://doi.org/10.3390/v12040450), indexed in Pubmed: [32316091](https://pubmed.ncbi.nlm.nih.gov/32316091/).
2. Campo MS. Animal models of papillomavirus pathogenesis. *Virus Res*. 2002; 89(2): 249–261, doi: [10.1016/s0168-1702\(02\)00193-4](https://doi.org/10.1016/s0168-1702(02)00193-4), indexed in Pubmed: [12445664](https://pubmed.ncbi.nlm.nih.gov/12445664/).
3. Carper MB, Troutman S, Wagner BL, et al. An immunocompetent mouse model of HPV16(+) head and neck squamous cell carcinoma. *Cell Rep*. 2019; 29(6): 1660–1674.e7, doi: [10.1016/j.celrep.2019.10.005](https://doi.org/10.1016/j.celrep.2019.10.005), indexed in Pubmed: [31693903](https://pubmed.ncbi.nlm.nih.gov/31693903/).
4. Chaturvedi AK, Engels EA, Pfeiffer RM, et al. Human papillomavirus and rising oropharyngeal cancer incidence in the United States. *J Clin Oncol*. 2011; 29(32): 4294–4301, doi: [10.1200/JCO.2011.36.4596](https://doi.org/10.1200/JCO.2011.36.4596), indexed in Pubmed: [21969503](https://pubmed.ncbi.nlm.nih.gov/21969503/).
5. Chen PN, Chen XY, Chen GX, et al. Squamous-columnar junction of Von Ebner's glands may be a significant origin of squamous cell carcinomas in the base of the tongue. *Front Oncol*. 2022; 12: 1029404, doi: [10.3389/fonc.2022.1029404](https://doi.org/10.3389/fonc.2022.1029404), indexed in Pubmed: [36465343](https://pubmed.ncbi.nlm.nih.gov/36465343/).
6. de Martel C, Plummer M, Vignat J, et al. Worldwide burden of cancer attributable to HPV by site, country and HPV type. *Int J Cancer*. 2017; 141(4): 664–670, doi: [10.1002/ijc.30716](https://doi.org/10.1002/ijc.30716), indexed in Pubmed: [28369882](https://pubmed.ncbi.nlm.nih.gov/28369882/).
7. de Oliveira Neto CP, Medeiros-Fonseca B, Estêvão D, et al. Differential incidence of tongue base cancer in male and female HPV16-transgenic mice: role of female sex hormone receptors. *Pathogens*. 2021; 10(10), doi: [10.3390/pathogens10101224](https://doi.org/10.3390/pathogens10101224), indexed in Pubmed: [34684173](https://pubmed.ncbi.nlm.nih.gov/34684173/).
8. Faraji F, Zaidi M, Fakhry C, et al. Molecular mechanisms of human papillomavirus-related carcinogenesis in head and neck cancer. *Microbes Infect*. 2017; 19(9-10): 464–475, doi: [10.1016/j.micinf.2017.06.001](https://doi.org/10.1016/j.micinf.2017.06.001), indexed in Pubmed: [28619685](https://pubmed.ncbi.nlm.nih.gov/28619685/).
9. Glickman JN, Chen YY, Wang HH, et al. Phenotypic characteristics of a distinctive multilayered epithelium suggests that it is a precursor in the development of Barrett's esophagus. *Am J Surg Pathol*. 2001; 25(5): 569–578, doi: [10.1097/00000478-200105000-00002](https://doi.org/10.1097/00000478-200105000-00002), indexed in Pubmed: [11342767](https://pubmed.ncbi.nlm.nih.gov/11342767/).
10. Gumus R, Capik O, Gundogdu B, et al. Low vitamin D and high cholesterol facilitate oral carcinogenesis in 4NQO-induced rat models via regulating glycolysis. *Oral Dis*. 2023; 29(3): 978–989, doi: [10.1111/odi.14117](https://doi.org/10.1111/odi.14117), indexed in Pubmed: [34954855](https://pubmed.ncbi.nlm.nih.gov/34954855/).
11. Herfs M, Yamamoto Y, Laury A, et al. A discrete population of squamocolumnar junction cells implicated in the pathogenesis of cervical cancer. *Proc Natl Acad Sci U S A*. 2012; 109(26): 10516–10521, doi: [10.1073/pnas.1202684109](https://doi.org/10.1073/pnas.1202684109), indexed in Pubmed: [22689991](https://pubmed.ncbi.nlm.nih.gov/22689991/).
12. Jiang M, Li H, Zhang Y, et al. Transitional basal cells at the squamous-columnar junction generate Barrett's esophagus. *Nature*. 2017; 550(7677): 529–533, doi: [10.1038/nature24269](https://doi.org/10.1038/nature24269), indexed in Pubmed: [29019984](https://pubmed.ncbi.nlm.nih.gov/29019984/).
13. Johnson DE, Burtneß B, Leemans CR, et al. Head and neck squamous cell carcinoma. *Nat Rev Dis Primers*. 2020; 6(1): 92, doi: [10.1038/s41572-020-00224-3](https://doi.org/10.1038/s41572-020-00224-3), indexed in Pubmed: [33243986](https://pubmed.ncbi.nlm.nih.gov/33243986/).
14. Jung HS, Akita K, Kim JY. Spacing patterns on tongue surface-gustatory papilla. *Int J Dev Biol*. 2004; 48(2-3): 157–161, doi: [10.1387/ijdb.15272380](https://doi.org/10.1387/ijdb.15272380), indexed in Pubmed: [15272380](https://pubmed.ncbi.nlm.nih.gov/15272380/).
15. Lambert PF. Transgenic mouse models of tumor virus action. *Annu Rev Virol*. 2016; 3(1): 473–489, doi: [10.1146/annurev-virology-100114-054908](https://doi.org/10.1146/annurev-virology-100114-054908), indexed in Pubmed: [27741405](https://pubmed.ncbi.nlm.nih.gov/27741405/).
16. Lechner M, Liu J, Masterson L, et al. HPV-associated oropharyngeal cancer: epidemiology, molecular biology and clinical management. *Nat Rev Clin Oncol*. 2022; 19(5):

- 306–327, doi: [10.1038/s41571-022-00603-7](https://doi.org/10.1038/s41571-022-00603-7), indexed in Pubmed: [35105976](https://pubmed.ncbi.nlm.nih.gov/35105976/).
17. Li H, Jing X, Yu J, et al. A combination of cytokeratin 5/6, p63, p40 and MUC5AC are useful for distinguishing squamous cell carcinoma from adenocarcinoma of the cervix. *Diagn Pathol.* 2020; 15(1): 104, doi: [10.1186/s13000-020-01018-7](https://doi.org/10.1186/s13000-020-01018-7), indexed in Pubmed: [32843061](https://pubmed.ncbi.nlm.nih.gov/32843061/).
 18. Maldonado JO, Beach ME, Wang Y, et al. HCV infection alters salivary gland histology and saliva composition. *J Dent Res.* 2022; 101(5): 534–541, doi: [10.1177/00220345211049395](https://doi.org/10.1177/00220345211049395), indexed in Pubmed: [35045743](https://pubmed.ncbi.nlm.nih.gov/35045743/).
 19. Maru Y, Kawata A, Taguchi A, et al. Establishment and molecular phenotyping of organoids from the squamo-columnar junction region of the uterine cervix. *Cancers (Basel).* 2020; 12(3), doi: [10.3390/cancers12030694](https://doi.org/10.3390/cancers12030694), indexed in Pubmed: [32183493](https://pubmed.ncbi.nlm.nih.gov/32183493/).
 20. Marur S, D'Souza G, Westra WH, et al. HPV-associated head and neck cancer: a virus-related cancer epidemic. *Lancet Oncol.* 2010; 11(8): 781–789, doi: [10.1016/S1470-2045\(10\)70017-6](https://doi.org/10.1016/S1470-2045(10)70017-6), indexed in Pubmed: [20451455](https://pubmed.ncbi.nlm.nih.gov/20451455/).
 21. McBride AA. Mechanisms and strategies of papillomavirus replication. *Biol Chem.* 2017; 398(8): 919–927, doi: [10.1515/hsz-2017-0113](https://doi.org/10.1515/hsz-2017-0113), indexed in Pubmed: [28315855](https://pubmed.ncbi.nlm.nih.gov/28315855/).
 22. Mirkovic J, Howitt BE, Roncarati P, et al. Carcinogenic HPV infection in the cervical squamo-columnar junction. *J Pathol.* 2015; 236(3): 265–271, doi: [10.1002/path.4533](https://doi.org/10.1002/path.4533), indexed in Pubmed: [25782708](https://pubmed.ncbi.nlm.nih.gov/25782708/).
 23. Morbini P, Capello GL, Alberizzi P, et al. Markers of squamocolumnar junction cells in normal tonsils and oropharyngeal cancer with and without HPV infection. *Histol Histopathol.* 2015; 30(7): 833–839, doi: [10.14670/HH-11-590](https://doi.org/10.14670/HH-11-590), indexed in Pubmed: [25644820](https://pubmed.ncbi.nlm.nih.gov/25644820/).
 24. Näsman A, Du J, Dalianis T. A global epidemic increase of an HPV-induced tonsil and tongue base cancer - potential benefit from a pan-gender use of HPV vaccine. *J Intern Med.* 2020; 287(2): 134–152, doi: [10.1111/joim.13010](https://doi.org/10.1111/joim.13010), indexed in Pubmed: [31733108](https://pubmed.ncbi.nlm.nih.gov/31733108/).
 25. O'Sullivan B, Huang SH, Su J, et al. Development and validation of a staging system for HPV-related oropharyngeal cancer by the International Collaboration on Oropharyngeal cancer Network for Staging (ICON-S): a multicentre cohort study. *Lancet Oncol.* 2016; 17(4): 440–451, doi: [10.1016/S1470-2045\(15\)00560-4](https://doi.org/10.1016/S1470-2045(15)00560-4), indexed in Pubmed: [26936027](https://pubmed.ncbi.nlm.nih.gov/26936027/).
 26. Parés D, Mullerat J, Pera M. Neoplasia intraepitelial anal. *Med Clín.* 2006; 127(19): 749–755, doi: [10.1157/13095527](https://doi.org/10.1157/13095527), indexed in Pubmed: [17198654](https://pubmed.ncbi.nlm.nih.gov/17198654/).
 27. Peng S, Xing D, Ferrall L, et al. Development of a spontaneous HPV16 E6/E7-expressing head and neck squamous cell carcinoma in HLA-A2 transgenic mice. *mBio.* 2022; 13(1): e0325221, doi: [10.1128/mbio.03252-21](https://doi.org/10.1128/mbio.03252-21), indexed in Pubmed: [35089069](https://pubmed.ncbi.nlm.nih.gov/35089069/).
 28. Porcheri C, Mitsiadis TA. Physiology, pathology and regeneration of salivary glands. *Cells.* 2019; 8(9), doi: [10.3390/cells8090976](https://doi.org/10.3390/cells8090976), indexed in Pubmed: [31455013](https://pubmed.ncbi.nlm.nih.gov/31455013/).
 29. Rathore K, Alexander M, Cekanova M. Piroxicam inhibits Masitinib-induced cyclooxygenase 2 expression in oral squamous cell carcinoma cells in vitro. *Transl Res.* 2014; 164(2): 158–168, doi: [10.1016/j.trsl.2014.02.002](https://doi.org/10.1016/j.trsl.2014.02.002), indexed in Pubmed: [24631063](https://pubmed.ncbi.nlm.nih.gov/24631063/).
 30. Redman RS. Morphologic diversity of the minor salivary glands of the rat: fertile ground for studies in gene function and proteomics. *Biotech Histochem.* 2012; 87(4): 273–287, doi: [10.3109/10520295.2011.639719](https://doi.org/10.3109/10520295.2011.639719), indexed in Pubmed: [22149361](https://pubmed.ncbi.nlm.nih.gov/22149361/).
 31. Van Dyne EA, Henley SJ, Saraiya M, et al. Trends in human papillomavirus-associated cancers — United States, 1999–2015. *MMWR Morb Mortal Wkly Rep.* 2018; 67(33): 918–924, doi: [10.15585/mmwr.mm6733a2](https://doi.org/10.15585/mmwr.mm6733a2), indexed in Pubmed: [30138307](https://pubmed.ncbi.nlm.nih.gov/30138307/).
 32. Viarisio D, Gissmann L, Tommasino M. Human papillomaviruses and carcinogenesis: well-established and novel models. *Curr Opin Virol.* 2017; 26: 56–62, doi: [10.1016/j.coviro.2017.07.014](https://doi.org/10.1016/j.coviro.2017.07.014), indexed in Pubmed: [28778034](https://pubmed.ncbi.nlm.nih.gov/28778034/).
 33. Yang EJ, Quick MC, Hanamornroongruang S, et al. Microanatomy of the cervical and anorectal squamocolumnar junctions: a proposed model for anatomical differences in HPV-related cancer risk. *Mod Pathol.* 2015; 28(7): 994–1000, doi: [10.1038/modpathol.2015.54](https://doi.org/10.1038/modpathol.2015.54), indexed in Pubmed: [25975286](https://pubmed.ncbi.nlm.nih.gov/25975286/).